Engineering Science and Technology, an International Journal 18 (2015) 309–317

HOSTED BY

Contents lists available at ScienceDirect

Engineering Science and Technology, an International Journal

journal homepage: http://www.elsevier.com/locate/jestch

Full length article

Unsteady MHD free convection flow of Casson fluid past over an oscillating vertical plate embedded in a porous medium

Asma Khalid [a, c], Ilyas Khan [b], Arshad Khan [c], Sharidan Shafie [c, *]

[a] Department of Mathematics, SBK Women's University, Quetta 87300, Pakistan
[b] College of Engineering Majmaah University, Majmaah 11952, Saudi Arabia
[c] Department of Mathematical Sciences, Faculty of Science, Universiti Teknologi Malaysia, Skudai 81310 UTM, Malaysia

ARTICLE INFO

Article history:
Received 2 October 2014
Received in revised form
10 November 2014
Accepted 2 December 2014
Available online 20 February 2015

Keywords:
Casson fluid
MHD flow
Porous medium
Free convection
Exact solutions

ABSTRACT

This article studies the unsteady MHD free flow of a Casson fluid past an oscillating vertical plate with constant wall temperature. The fluid is electrically conducting and passing through a porous medium. This phenomenon is modelled in the form of partial differential equations with initial and boundary conditions. Some suitable non-dimensional variables are introduced. The corresponding non-dimensional equations with conditions are solved using the Laplace transform technique. Exact solutions for velocity and energy are obtained. They are expressed in simple forms in terms of exponential and complementary error functions of Gauss. It is found that they satisfy governing equations and corresponding conditions, and are reduced to similar solutions for Newtonian fluids as a special case. Expressions for skin-friction and Nusselt number are also evaluated. Computations are carried out and the results are analysed for emerging flow parameters.

1. Introduction

The study of magnetohydrodynamic (MHD) flow of non-Newtonian fluid in a porous medium has attracted the attentions of many researchers. Of course, it is due to the fact that such phenomenons are mostly found in the optimization of solidification processes of metals and metal alloys, the geothermal sources investigation and nuclear fuel debris treatment. However, non-Newtonian fluids are subtle compare to Newtonian fluids. Indeed, the resulting equations of non-Newtonian fluids give highly nonlinear differential equations which are usually difficult to solve. These equations add further complexities when MHD flows in a porous space have been taken into account. Ample applications for the MHD flows of non-Newtonian fluids in a porous medium are encountered in irrigation problems, heat-storage beds, biological systems, process of petroleum, textile, paper and polymer composite industries. Numerous studies have been presented on various aspects of MHD flows of non-Newtonian fluid flows passing through a porous medium. One may refer to some recent investigations [1–5].

On the other hand, convection flow arises in many physical situations such as in the cooling of nuclear reactors and in the study of environmental heat transfer processes amongst others. Convection is of three types namely free, mixed and force. Amongst them free convection is important in many engineering applications including an example of automatic control systems consist of electrical and electronic components, regularly subjected to periodic heating and cooled by free convection process. Some recent studies containing the free convection phenomenon can be found in [6–10] and the references therein. Besides that the work on free convection for non-Newtonian fluids when exact solutions are needed is limited. Further, when MHD and porosity effects are added to the governing equations then even such solutions are scarce. Farhad et al. [11] obtained closed form solutions for unsteady free convection flow of a second grade fluid over an oscillating vertical plate. Khan et al. [12] developed exact solutions for unsteady free convection flow of Walters'-B fluid. Samiulhaq et al. [13] analysed unsteady MHD free convection flow of a second grade fluid in a porous medium with ramped wall temperature.

In nature, some non-Newtonian fluids behave like elastic solid that is, no flow occur with small shear stress. Casson fluid is one of such fluids. This fluid has distinct features and is quite famous recently. Casson fluid model was introduced by Casson in 1959 for the prediction of the flow behaviour of pigment-oil suspensions

* Corresponding author. Tel.: +60 137731773.
E-mail address: sharidan@utm.com (S. Shafie).
Peer review under responsibility of Karabuk University.

http://dx.doi.org/10.1016/j.jestch.2014.12.006

[14]. So, for the flow, the shear stress magnitude of Casson fluid needs to exceed the yield shear stress, otherwise the fluid behaves as a rigid body. This type of fluids can be marked as a purely viscous fluid with high viscosity [15]. Casson model is based on a structure model of the interactive behavior of solid and liquid phases of a two-phase suspension. Some famous examples of Casson fluid include jelly, tomato sauce, honey, soup and concentrated fruit juices. Human blood can also be treated as Casson fluid due to the presence of several substances such as protein, fibrinogen, globulin in aqueous base plasma and human red blood cells [16,17].

In the earlier studies on Casson fluid, Boyd et al. [18] discussed the steady and oscillatory flow of blood by taking into account Casson fluid whereas Fredrickson [19] investigated its steady flow in a tube. The peristaltic flow of a Casson fluid in a two-dimensional channel is described by Mernone et al. [20]. Mustafa et al. [21] studied the unsteady boundary layer flow and heat transfer of a Casson fluid over a moving flat plate with a parallel free stream using homotopy analysis method (HAM). Mixed convection stagnation-point flow of Casson fluid with convective boundary conditions is examined by Hayat et al. [22]. Shaw et al. [23] discussed the effect of non-Newtonian characteristics of blood on magnetic targeting in the impermeable micro-vessel. Magnetic targeting in the impermeable microvessel with two-phase fluid model-Non-Newtonian characteristic of blood carried out by Shaw and Murthy [24]. Pulsatile Casson fluid flow through a stenosed bifurcated artery also studied by Shaw et al. [25]. The effects of thermal radiation on Casson fluid flow and heat transfer over an unsteady stretching surface subjected to suction/blowing has been developed by Mukhopadhyay [26]. Bhattacharyya [27] constructed the boundary layer stagnation-point flow of Casson fluid and heat transfer towards a shrinking/stretching sheet. Mukhopadhyay et al. [28] also analysed the Casson fluid flow over an unsteady stretching surface followed by Pramanik [29] where he studied the Casson fluid flow and heat transfer past an exponentially porous stretching surface in the presence of thermal radiation.

In all of the above studies the solutions of Casson fluid are either obtained by using approximate method or by any numerical scheme. There are very few cases in which the exact analytical solutions of Casson fluid are obtained. These solutions are even rare when Casson fluid in free convection flow with constant wall temperature is considered. On the other hand, the flow of Casson fluids (such as drilling muds, clay coatings and other suspensions, certain oils and greases, polymer melts, blood and many emulsions), in the presence of heat transfer is an important research area due to its relevance in the optimized processing of chocolate, toffee, and other foodstuffs [21,30–32].

The purpose of the present investigation is two-fold. Firstly, it incorporates the effects of magnetic field by considering the fluid to be electrically conducting. Secondly, the fluid is considered in a porous medium. More exactly, the present work concentres on unsteady MHD free convection flow of a Casson fluid over a vertical plate embedded in a porous medium. Exact solutions when the plate performs sine and cosine oscillations with constant wall temperature are obtained by using the Laplace transform technique [33–36]. Analytical and numerical results for skin-friction and Nusselt number are provided. Graphical results are presented and discussed for various physical parameters entering into the problem.

2. Formulation of the problem

We consider Casson fluid over an infinite vertical flat plate embedded in a saturated porous medium. The flow being confined to $y>0$, where y is the coordinate measured in the normal direction to the plate. The fluid is assumed to be electrically conducting with a uniform magnetic field B of strength B_0, applied in a direction perpendicular to the plate. The magnetic Reynolds number is assumed to be small enough to neglect the effects of applied magnetic field. Initially, for time $t=0$, both the fluid and the plate are at rest with uniform temperature. At time $t=0^+$ the plate begins to oscillate in its plane $(y=0)$ according to

$$\mathrm{V}=UH(t)\cos(\omega t)\mathbf{i};\ \text{or}\ \mathrm{V}=U\sin(\omega t)\mathbf{i};\ t>0, \tag{1}$$

where the constant U is the amplitude of the plate oscillations, $H(t)$ is the unit step function, $\mathbf{i}$ is the unit vector in the vertical flow direction and ω is the frequency of oscillation of the plate. At the same time, the plate temperature is raised to T_w which is thereafter maintained constant.

The rheological equation of state for the Cauchy stress tensor of Casson fluid is written as, (see [22,26,27,28,32])

$$\tau=\tau_0+\mu\gamma^{\bullet},$$

or

$$\tau_{ij}=\begin{cases}2\left(\mu_B+\dfrac{p_y}{\sqrt{2\pi}}\right)e_{ij}, & \pi>\pi_c\\ 2\left(\mu_B+\dfrac{p_y}{\sqrt{2\pi_c}}\right)e_{ij}, & \pi<\pi_c\end{cases},$$

where $\pi=e_{ij}\,e_{ij}$ and e_{ij} is the $(i,\,j)^{ih}$ component of the deformation rate, π is the product of the component of deformation rate with itself, π_c is a critical value of this product based on the non-Newtonian model, μ_B is plastic dynamic viscosity of the non-Newtonian fluid and p_y is yield stress of fluid. Before we derive the governing equations, the following assumptions are made, rigid plate, incompressible flow, unsteady flow, unidirectional flow, one dimensional flow, non-Newtonian flow, free convection, oscillating vertical plate and viscous dissipation term in the energy equation is neglected. Under these conditions we get the following set of partial differential equations

$$\rho\frac{\partial u}{\partial t}=\mu_B\left(1+\frac{1}{\gamma}\right)\frac{\partial^2 u}{\partial y^2}-\sigma B_0^2u-\frac{\mu\varphi}{k_1}u+\rho g\beta(T-T_\infty), \tag{2}$$

$$\rho c_p\frac{\partial T}{\partial t}=k\frac{\partial^2 T}{\partial y^2}, \tag{3}$$

together with initial and boundary conditions

$$\begin{aligned}&t<0: u=0, T=T_\infty \text{ for all } y>0,\\ &t\geq 0: u=UH(t)\cos(\omega t) \text{ or } u=U\sin(\omega t), T=T_w \text{ at } y=0,\\ &u\to 0, T\to T_\infty \text{ as } y\to\infty,\end{aligned} \tag{4}$$

where $u, t, T, \mu_B, \gamma, \rho, g, \beta, c_p, k, \sigma, \phi,$ and k_1 are the velocity of the fluid in $x-$ direction, time, temperature, plastic dynamic viscosity, Casson parameter, the constant density, the gravitational acceleration, volumetric coefficient of thermal expansion, specific heat at constant pressure and thermal conductivity, electric conductivity of the fluid, porosity and permeability of the fluid, respectively.

We introduce the following dimensionless variables

$$u^*=\frac{u}{U}, y^*=\frac{U}{\nu}y, t^*=\frac{U^2}{\nu}t, \theta=\frac{T-T_\infty}{T_w-T_\infty}, \omega^*=\frac{\omega\nu}{U^2}, \tau^*=\frac{\tau}{\rho u^2}, \tag{5}$$

into Equations. (2)–(4), and we get (* symbols are dropped for simplicity)

$$\frac{\partial u}{\partial t}=\left(1+\frac{1}{\gamma}\right)\frac{\partial^2 u}{\partial y^2}-M^2u^*-\frac{1}{K}u^*+Gr\theta, \tag{6}$$

$$\mathrm{Pr}\frac{\partial\theta}{\partial t}=\frac{\partial^2\theta}{\partial y^2}, \tag{7}$$

with associated initial and boundary conditions

$$\begin{aligned} &t<0: u=0, \theta=0 \text{ for all } y>0,\\ &t\geq 0: u=H(t)\cos(\omega t) \text{ or } u=\sin(\omega t), \theta=1 \text{ at } y=0,\\ &u\to 0, \theta\to 0 \text{ as } y\to\infty, \end{aligned} \tag{8}$$

$$\theta(y,t)=erfc\left(\frac{y}{2}\sqrt{\frac{\mathrm{Pr}}{t}}\right), \tag{11}$$

$$\begin{aligned} u_c(y,t)=&\frac{H(t)}{4}e^{-i\omega t}\left[e^{-y\sqrt{a(L-i\omega)}}erfc\left(\frac{y}{2}\sqrt{\frac{a}{t}}-\sqrt{(L-i\omega)t}\right)+e^{y\sqrt{a(L-i\omega)}}erfc\left(\frac{y}{2}\sqrt{\frac{a}{t}}+\sqrt{(L-i\omega)t}\right)\right]\\ &+\frac{H(t)}{4}e^{i\omega t}\left[e^{-y\sqrt{a(L+i\omega)}}erfc\left(\frac{y}{2}\sqrt{\frac{a}{t}}-\sqrt{(L+i\omega)t}\right)+e^{y\sqrt{a(L+i\omega)}}erfc\left(\frac{y}{2}\sqrt{\frac{a}{t}}+\sqrt{(L+i\omega)t}\right)\right]\\ &+\frac{ab}{2}\left[\left(\left(t-\frac{y}{2}\sqrt{\frac{a}{L}}\right)e^{-y\sqrt{aL}}erfc\left(\frac{y}{2}\sqrt{\frac{a}{t}}\right)-\sqrt{Lt}\right)+\left(\left(t+\frac{y}{2}\sqrt{\frac{a}{L}}\right)e^{-y\sqrt{aL}}erfc\left(\frac{y}{2}\sqrt{\frac{a}{t}}\right)+\sqrt{Lt}\right)\right]\\ &-ab\left[\left(t+\frac{\mathrm{Pr}y^2}{2}\right)erfc\left(\frac{y}{2}\sqrt{\frac{\mathrm{Pr}}{t}}\right)-y\sqrt{\mathrm{Pr}}\sqrt{\frac{t}{\pi}}e^{-\frac{\mathrm{Pr}y^2}{4t}}\right]. \end{aligned} \tag{12}$$

The subscript "c" on the left side of Equation (12) stands for the cosine oscillations of the plate. Similarly, the velocity corresponding to the sine oscillations of the plate is given by

$$\begin{aligned} u_s(y,t)=&\frac{1}{4i}e^{-i\omega t}\left[e^{-y\sqrt{a(L-i\omega)}}erfc\left(\frac{y}{2}\sqrt{\frac{a}{t}}-\sqrt{(L-i\omega)t}\right)+e^{y\sqrt{a(L-i\omega)}}erfc\left(\frac{y}{2}\sqrt{\frac{a}{t}}+\sqrt{(L-i\omega)t}\right)\right]\\ &+\frac{1}{4i}e^{i\omega t}\left[e^{-y\sqrt{a(L+i\omega)}}erfc\left(\frac{y}{2}\sqrt{\frac{a}{t}}-\sqrt{(L+i\omega)t}\right)+e^{y\sqrt{a(L+i\omega)}}erfc\left(\frac{y}{2}\sqrt{\frac{a}{t}}+\sqrt{(L+i\omega)t}\right)\right]\\ &+\frac{ab}{2}\left[\left(\left(t-\frac{y}{2}\sqrt{\frac{a}{L}}\right)e^{-y\sqrt{aL}}erfc\left(\frac{y}{2}\sqrt{\frac{a}{t}}\right)-\sqrt{Lt}\right)+\left(\left(t+\frac{y}{2}\sqrt{\frac{a}{L}}\right)e^{-y\sqrt{aL}}erfc\left(\frac{y}{2}\sqrt{\frac{a}{t}}\right)+\sqrt{Lt}\right)\right]\\ &-ab\left[\left(t+\frac{\mathrm{Pr}y^2}{2}\right)erfc\left(\frac{y}{2}\sqrt{\frac{\mathrm{Pr}}{t}}\right)-y\sqrt{\mathrm{Pr}}\sqrt{\frac{t}{\pi}}e^{-\frac{\mathrm{Pr}y^2}{4t}}\right], \end{aligned} \tag{13}$$

where

$$\mathrm{Pr}=\frac{\mu c_p}{k}, M^2=\frac{\sigma\upsilon B_0^2}{\rho U^2}, \frac{1}{K}=\frac{\upsilon\varphi^2}{k_1U^2}, Gr=\frac{\upsilon g\beta(T_w-T_\infty)}{U^3} \text{ and } \gamma=\frac{\mu_B\sqrt{2\pi_c}}{P_y},$$

here Pr is the Prandtl number, M is the magnetic parameter called Hartmann number, K is the dimensionless permeability parameter, Gr is the Grashof number and γ is the Casson parameter.

3. Exact solutions

In order to find exact solutions of the system of Equations. (6)–(8), we use the Laplace transform technique. Thus by taking the Laplace transforms of Equations. (6) and (7), using initial and boundary conditions (8), we get the following solutions in the transformed (y,q) plane

$$\overline{\theta}(y,q)=\frac{1}{q}e^{-y\sqrt{\mathrm{Pr}q}}, \tag{9}$$

$$\overline{u}(y,q)=\frac{q}{q^2+\omega^2}e^{-y\sqrt{a(q+L)}}+\frac{ab}{q^2}e^{-y\sqrt{a(q+L)}}-\frac{ab}{q^2}e^{-y\sqrt{\mathrm{Pr}q}}. \tag{10}$$

The inverse Laplace transforms of Equations. (9) and (10) are obtained as follows:

where

$$a=\frac{\gamma}{1+\gamma}, b=\frac{Gr}{\mathrm{Pr}-1}.$$

Note that the above solutions for velocity are only valid for $\mathrm{Pr}\neq 1$. Moreover, the solution for $\mathrm{Pr}=1$ can be easily obtained by putting $\mathrm{Pr}=1$ into Equation (7), and follow a similar procedure as discussed above. The obtained solutions for cosine and sine oscillations of the plate when $\mathrm{Pr}=1$ are

$$\begin{aligned} u_c(y,t)=&\frac{H(t)}{4}e^{-i\omega t}\left[e^{-y\sqrt{a(L-i\omega)}}erfc\left(\frac{y}{2}\sqrt{\frac{a}{t}}-\sqrt{(L-i\omega)t}\right)\right.\\ &\left.+e^{y\sqrt{a(L-i\omega)}}erfc\left(\frac{y}{2}\sqrt{\frac{a}{t}}+\sqrt{(L-i\omega)t}\right)\right]\\ &+\frac{H(t)}{4}e^{i\omega t}\left[e^{-y\sqrt{a(L+i\omega)}}erfc\left(\frac{y}{2}\sqrt{\frac{a}{t}}-\sqrt{(L+i\omega)t}\right)\right.\\ &\left.+e^{y\sqrt{a(L+i\omega)}}erfc\left(\frac{y}{2}\sqrt{\frac{a}{t}}+\sqrt{(L+i\omega)t}\right)\right]\\ &-\frac{a\,Gr\,y}{2}\left[2\sqrt{\frac{t}{\pi}}e^{-\frac{y^2}{4t}}-y\,\mathrm{erf}\,c\left(\frac{y}{2\sqrt{t}}\right)\right], \end{aligned} \tag{14}$$

$$u_s(y,t) = \frac{1}{4i}e^{-i\omega t}\left[e^{-y\sqrt{a(L-i\omega)}}erfc\left(\frac{y}{2}\sqrt{\frac{a}{t}}-\sqrt{(L-i\omega)t}\right)+e^{y\sqrt{a(L-i\omega)}}erfc\left(\frac{y}{2}\sqrt{\frac{a}{t}}+\sqrt{(L-i\omega)t}\right)\right]$$
$$+\frac{1}{4i}e^{i\omega t}\left[e^{-y\sqrt{a(L+i\omega)}}erfc\left(\frac{y}{2}\sqrt{\frac{a}{t}}-\sqrt{(L+i\omega)t}\right)+e^{y\sqrt{a(L+i\omega)}}erfc\left(\frac{y}{2}\sqrt{\frac{a}{t}}+\sqrt{(L+i\omega)t}\right)\right] \quad (15)$$
$$-\frac{a\,Gr\,y}{2}\left[2\sqrt{\frac{t}{\pi}}e^{-\frac{y^2}{4t}}-y\,\mathrm{erf}\,c\left(\frac{y}{2\sqrt{t}}\right)\right].$$

Note that in Equations. (12) and (13), the first two terms in each equation account the contribution from mechanical parts while the last two terms show the thermal effects. On the other hand in Equations. (14) and (15), the last term in each equation shows the contribution from the thermal part.

4.1. Solutions for large values of γ

By taking $\gamma \to \infty$ into Equations. (12) and (13), the corresponding solutions for viscous fluid can be obtained as a special case:

$$u_c(y,t) = \frac{H(t)}{4}e^{-i\omega t}\left[e^{-y\sqrt{(L-i\omega)}}erfc\left(\frac{y}{2}\sqrt{\frac{1}{t}}-\sqrt{(L-i\omega)t}\right)+e^{y\sqrt{(L-i\omega)}}erfc\left(\frac{y}{2}\sqrt{\frac{1}{t}}+\sqrt{(L-i\omega)t}\right)\right]$$
$$+\frac{H(t)}{4}e^{i\omega t}\left[e^{-y\sqrt{(L+i\omega)}}erfc\left(\frac{y}{2}\sqrt{\frac{1}{t}}-\sqrt{(L+i\omega)t}\right)+e^{y\sqrt{(L+i\omega)}}erfc\left(\frac{y}{2}\sqrt{\frac{1}{t}}+\sqrt{(L+i\omega)t}\right)\right]$$
$$+\frac{b}{2}\left[\left(\left(t-\frac{y}{2}\sqrt{\frac{1}{L}}\right)e^{-y\sqrt{L}}erfc\left(\frac{y}{2}\sqrt{\frac{1}{t}}\right)-\sqrt{Lt}\right)+\left(\left(t+\frac{y}{2}\sqrt{\frac{1}{L}}\right)e^{-y\sqrt{L}}erfc\left(\frac{y}{2}\sqrt{\frac{1}{t}}\right)+\sqrt{Lt}\right)\right] \quad (18)$$
$$-b\left[\left(t+\frac{\mathrm{Pr}y^2}{2}\right)erfc\left(\frac{y}{2}\sqrt{\frac{\mathrm{Pr}}{t}}\right)-y\sqrt{\mathrm{Pr}}\sqrt{\frac{t}{\pi}}e^{-\frac{\mathrm{Pr}y^2}{4t}}\right],$$

3.1. Nusselt number and skin-friction

Expressions for Nusselt number and skin-friction are calculated from Equations. (11) and (12) using the relations

$$\mathrm{Nu} = -\frac{\nu}{U_0(T-T_\infty)}\left.\frac{\partial T^*}{\partial y^*}\right|_{y^*=0} = \sqrt{\frac{\mathrm{Pr}}{\pi t}}, \quad (16)$$

$$\tau = -\mu\left(1+\frac{1}{\gamma}\right)\left.\frac{\partial u}{\partial y}\right|_{y=0},$$

$$\tau = \frac{1}{2}\left[\frac{2\left[-e^{-Lt}H\sqrt{\frac{a}{t}}+ab\sqrt{\mathrm{Pr}}\sqrt{t}-abe^{-Lt}\sqrt{\frac{a}{t}}t+ab\sqrt{\frac{\mathrm{Pr}}{t}}t\right]}{\sqrt{\pi}}\right.$$
$$-ab\left[\sqrt{\frac{a}{L}}+2\sqrt{aLt}\right]\mathrm{erf}(\sqrt{Lt})$$
$$-e^{-i\omega t}H\left\{\sqrt{a(L-i\omega)}\,\mathrm{erf}(\sqrt{t(L-i\omega)}\right.$$
$$\left.\left.+e^{2it\omega}\sqrt{a(L+i\omega)}\,\mathrm{erf}(\sqrt{t(L+i\omega)})\right\}\right]. \quad (17)$$

4. Special cases

In order to underline the theoretical value of the general solutions (12) and (13) for velocity, as well as to gain physical insight of the flow regime, we consider some special cases whose technical relevance is well known in the literature.

$$u_s(y,t) = \frac{1}{4i}e^{-i\omega t}\left[e^{-y\sqrt{(L-i\omega)}}erfc\left(\frac{y}{2}\sqrt{\frac{1}{t}}-\sqrt{(L-i\omega)t}\right)\right.$$
$$\left.+e^{y\sqrt{(L-i\omega)}}erfc\left(\frac{y}{2}\sqrt{\frac{1}{t}}+\sqrt{(L-i\omega)t}\right)\right]$$
$$+\frac{1}{4i}e^{i\omega t}\left[e^{-y\sqrt{(L+i\omega)}}erfc\left(\frac{y}{2}\sqrt{\frac{1}{t}}-\sqrt{(L+i\omega)t}\right)\right.$$
$$\left.+e^{y\sqrt{(L+i\omega)}}erfc\left(\frac{y}{2}\sqrt{\frac{1}{t}}+\sqrt{(L+i\omega)t}\right)\right]$$
$$+\frac{b}{2}\left[\left(\left(t-\frac{y}{2}\sqrt{\frac{1}{L}}\right)e^{-y\sqrt{L}}erfc\left(\frac{y}{2}\sqrt{\frac{1}{t}}\right)-\sqrt{Lt}\right)\right.$$
$$\left.+\left(\left(t+\frac{y}{2}\sqrt{\frac{1}{L}}\right)e^{-y\sqrt{L}}erfc\left(\frac{y}{2}\sqrt{\frac{1}{t}}\right)+\sqrt{Lt}\right)\right]$$
$$-b\left[\left(t+\frac{\mathrm{Pr}y^2}{2}\right)erfc\left(\frac{y}{2}\sqrt{\frac{\mathrm{Pr}}{t}}\right)-y\sqrt{\mathrm{Pr}}\sqrt{\frac{t}{\pi}}e^{-\frac{\mathrm{Pr}y^2}{4t}}\right]. \quad (19)$$

4.2. Solutions for stokes first problem

By taking $\omega = 0$, which corresponds to impulsive motion of the plate, then Equations. (12) and (13), yield

$$u_c(y,t) = \frac{1}{2}H\left[e^{-y\sqrt{aL}}erfc\left(\frac{y}{2}\sqrt{\frac{a}{t}}-\sqrt{Lt}\right)+e^{y\sqrt{aL}}erfc\left(\frac{y}{2}\sqrt{\frac{a}{t}}+\sqrt{Lt}\right)\right] + \frac{ab}{2}\left[\left(\left(t-\frac{y}{2}\sqrt{\frac{a}{L}}\right)e^{-y\sqrt{aL}}erfc\left(\frac{y}{2}\sqrt{\frac{a}{t}}\right)-\sqrt{Lt}\right) + \left(\left(t+\frac{y}{2}\sqrt{\frac{a}{L}}\right)e^{-y\sqrt{aL}}erfc\left(\frac{y}{2}\sqrt{\frac{a}{t}}\right)+\sqrt{Lt}\right)\right] - ab\left[\left(t+\frac{\mathrm{Pry}^2}{2}\right)erfc\left(\frac{y}{2}\sqrt{\frac{\mathrm{Pr}}{t}}\right)-\frac{y\sqrt{\mathrm{Pr}}\sqrt{t}e^{-\frac{\mathrm{Pry}^2}{4t}}}{\sqrt{\pi}}\right], \tag{20}$$

respectively,

$$u_s(y,t) = \frac{1}{2i}H\left[e^{-y\sqrt{aL}}erfc\left(\frac{y}{2}\sqrt{\frac{a}{t}}-\sqrt{Lt}\right)+e^{y\sqrt{aL}}erfc\left(\frac{y}{2}\sqrt{\frac{a}{t}}+\sqrt{Lt}\right)\right] + \frac{ab}{2}\left[\left(\left(t-\frac{y}{2}\sqrt{\frac{a}{L}}\right)e^{-y\sqrt{aL}}erfc\left(\frac{y}{2}\sqrt{\frac{a}{t}}\right)-\sqrt{Lt}\right) + \left(\left(t+\frac{y}{2}\sqrt{\frac{a}{L}}\right)e^{-y\sqrt{aL}}erfc\left(\frac{y}{2}\sqrt{\frac{a}{t}}\right)+\sqrt{Lt}\right)\right] - ab\left[\left(t+\frac{\mathrm{Pry}^2}{2}\right)erfc\left(\frac{y}{2}\sqrt{\frac{\mathrm{Pr}}{t}}\right)-y\sqrt{\mathrm{Pr}}\frac{\sqrt{t}e^{-\frac{\mathrm{Pry}^2}{4t}}}{\sqrt{\pi}}\right]. \tag{21}$$

4.3. Absence of MHD and porosity effects: attend

The temperature distribution is not effected by MHD and porous medium, as it results from Equation (11). However, MHD and porosity have strong influence on velocity as it can be seen from the mechanical parts of Equations. (12) and (13). Thus in the absence of MHD ($M = 0$) and porous medium ($1/K = 0$), these equalities become

$$u_c(y,t) = \frac{H(t)}{4}e^{-i\omega t}\left[e^{-y\sqrt{a(-i\omega)}}erfc\left(\frac{y}{2}\sqrt{\frac{a}{t}}-\sqrt{(-i\omega)t}\right)+e^{y\sqrt{a(-i\omega)}}erfc\left(\frac{y}{2}\sqrt{\frac{a}{t}}+\sqrt{(-i\omega)t}\right)\right] + \frac{H(t)}{4}e^{i\omega t}\left[e^{-y\sqrt{a(i\omega)}}erfc\left(\frac{y}{2}\sqrt{\frac{a}{t}}-\sqrt{(i\omega)t}\right)+e^{y\sqrt{a(i\omega)}}erfc\left(\frac{y}{2}\sqrt{\frac{a}{t}}+\sqrt{(i\omega)t}\right)\right] + \frac{ab}{2}\left[\left(\left(t-\frac{y}{2}\sqrt{a}\right)e^{-y\sqrt{a}}erfc\left(\frac{y}{2}\sqrt{\frac{a}{t}}\right)-\sqrt{t}\right)+\left(\left(t+\frac{y}{2}\sqrt{a}\right)e^{-y\sqrt{a}}erfc\left(\frac{y}{2}\sqrt{\frac{a}{t}}\right)+\sqrt{t}\right)\right] - ab\left[\left(t+\frac{\mathrm{Pry}^2}{2}\right)erfc\left(\frac{y}{2}\sqrt{\frac{\mathrm{Pr}}{t}}\right)-y\sqrt{\mathrm{Pr}}\sqrt{\frac{t}{\pi}}e^{-\frac{\mathrm{Pry}^2}{4t}}\right], \tag{22}$$

$$u_s(y,t) = \frac{1}{4i}e^{-i\omega t}\left[e^{-y\sqrt{a(-i\omega)}}erfc\left(\frac{y}{2}\sqrt{\frac{a}{t}}-\sqrt{(-i\omega)t}\right)+e^{y\sqrt{a(-i\omega)}}erfc\left(\frac{y}{2}\sqrt{\frac{a}{t}}+\sqrt{(-i\omega)t}\right)\right] + \frac{1}{4i}e^{i\omega t}\left[e^{-y\sqrt{a(i\omega)}}erfc\left(\frac{y}{2}\sqrt{\frac{a}{t}}-\sqrt{(i\omega)t}\right)+e^{y\sqrt{a(i\omega)}}erfc\left(\frac{y}{2}\sqrt{\frac{a}{t}}+\sqrt{(i\omega)t}\right)\right] + \frac{ab}{2}\left[\left(\left(t-\frac{y}{2}\sqrt{a_1}\right)e^{-y\sqrt{a}}erfc\left(\frac{y}{2}\sqrt{\frac{a}{t}}\right)-\sqrt{t}\right)+\left(\left(t+\frac{y}{2}\sqrt{a}\right)e^{-y\sqrt{a}}erfc\left(\frac{y}{2}\sqrt{\frac{a}{t}}\right)+\sqrt{t}\right)\right] - ab\left[\left(t+\frac{\mathrm{Pry}^2}{2}\right)erfc\left(\frac{y}{2}\sqrt{\frac{\mathrm{Pr}}{t}}\right)-y\sqrt{\mathrm{Pr}}\sqrt{\frac{t}{\pi}}e^{-\frac{\mathrm{Pry}^2}{4t}}\right]. \tag{23}$$

4.4. Solution in the absence of mechanical effects

Let us now assume that the infinite plate is kept at rest all the time. In this case, the wall velocity of the fluid is zero for each real value of t and thus the mechanical component of velocity identically vanishes. Consequently, the velocity of the fluid $u(y,t)$ reduces to the thermal component of Equation (13). Its temperature as well as the surface heat transfer rate are given by the same equalities (11) and (16).

4.5. Solution in the absence of mechanical effects

In the last case, we assume that the flow is induced only due to bounding plate and the corresponding buoyancy forces are zero equivalently it shows the absence of free convection ($Gr = 0$) due to the differences in temperature gradient. This shows that the thermal parts of velocities in Equations (12) and (13) are zero. Hence the flow is only governed by the corresponding mechanical parts given by

$$u_c(y,t) = \frac{H(t)}{4}e^{-i\omega t}\left[e^{-y\sqrt{a(L-i\omega)}}erfc\left(\frac{y}{2}\sqrt{\frac{a}{t}}-\sqrt{(L-i\omega)t}\right)+e^{y\sqrt{a(L-i\omega)}}erfc\left(\frac{y}{2}\sqrt{\frac{a}{t}}+\sqrt{(L-i\omega)t}\right)\right] + \frac{H(t)}{4}e^{i\omega t}\left[e^{-y\sqrt{a(L+i\omega)}}erfc\left(\frac{y}{2}\sqrt{\frac{a}{t}}-\sqrt{(L+i\omega)t}\right)+e^{y\sqrt{a(L+i\omega)}}erfc\left(\frac{y}{2}\sqrt{\frac{a}{t}}+\sqrt{(L+i\omega)t}\right)\right], \tag{24}$$

$$u_s(y,t) = \frac{1}{4i}e^{-i\omega t}\left[e^{-y\sqrt{a(L-i\omega)}}erfc\left(\frac{y}{2}\sqrt{\frac{a}{t}}-\sqrt{(L-i\omega)t}\right)\right.$$
$$\left.+\,e^{y\sqrt{a(L-i\omega)}}erfc\left(\frac{y}{2}\sqrt{\frac{a}{t}}+\sqrt{(L-i\omega)t}\right)\right]$$
$$+\frac{1}{4i}e^{i\omega t}\left[e^{-y\sqrt{a(L+i\omega)}}erfc\left(\frac{y}{2}\sqrt{\frac{a}{t}}-\sqrt{(L+i\omega)t}\right)\right.$$
$$\left.+\,e^{y\sqrt{a(L+i\omega)}}erfc\left(\frac{y}{2}\sqrt{\frac{a}{t}}+\sqrt{(L+i\omega)t}\right)\right]. \quad (25)$$

Note that Equations (24) and (25) when $\gamma\to\infty$, are identical to those obtained by Fetecau et al. [31], see Equations (8) and (9). This fact is also shown in Fig. 10.

5. Results and discussion

In this section, the obtained exact solutions are studied numerically in order to determine the effects of several involved parameters such as Prandtl number Pr, Grashof number *Gr*, Casson parameter γ, magnetic parameter *M*, permeability of porous medium *K*, phase angle ωt and time *t*. Numerical values of skin-friction and Nusselt number are computed and presented in tables for different parameters. Physical sketch of the problem is shown in Fig. 1. Fig. 2 exhibits the velocity profiles for different values of Prandtl number Pr, when the other parameters are fixed. It is observed that velocity of the fluid decreases with increasing Prandtl number. Fig. 3 illustrates the profiles of velocity for different values of *Gr*. It is observed that velocity increases with increasing values of *Gr*. The flow is accelerated due to the enhancement in the buoyancy forces corresponding to the increasing values of Grashof number, i.e., free convection effects. The influence of Casson fluid parameter on velocity profiles is shown in Fig. 4. It is found that velocity decreases with increasing values of γ. It is important to note that an increase in Casson parameter makes the velocity boundary layer thickness shorter. It is further observed from this graph that when the Casson paramter γ is large enough i.e. $\gamma\to\infty$, the non-Newtonian behaviours disappear and the fluid purely behaves like a Newtonian fluid. Thus, the velocity boundary layer thickness for Casson fluid is larger than the Newtonian fluid. It occurs because of plasticity of Casson fluid. When Casson parameter decreases the plasticity of the fluid increases, which causes the

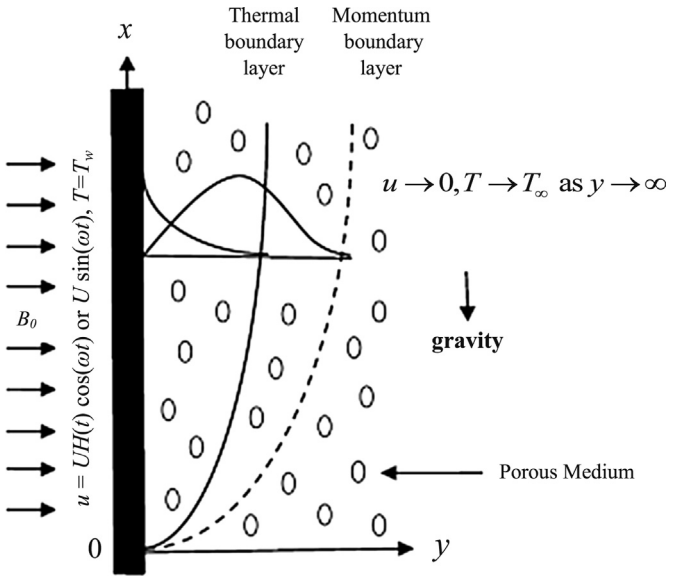

Fig. 1. Physical sketch of the problem.

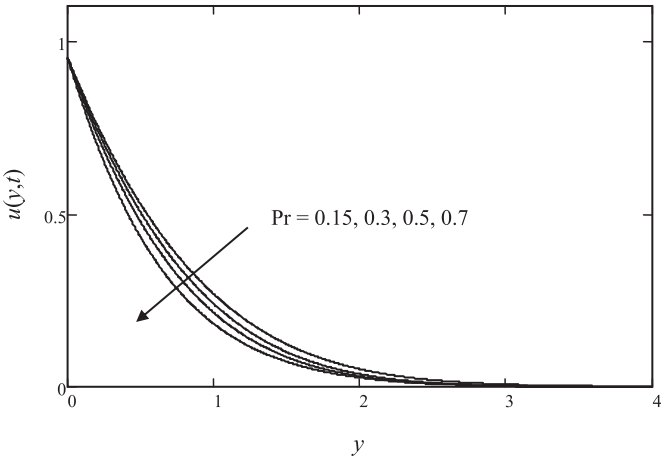

Fig. 2. Profiles of velocity for different values of Pr, when $M = 0.5, K = 0.2, \omega = \pi/4, t = 0.2$ and $Gr = 3$.

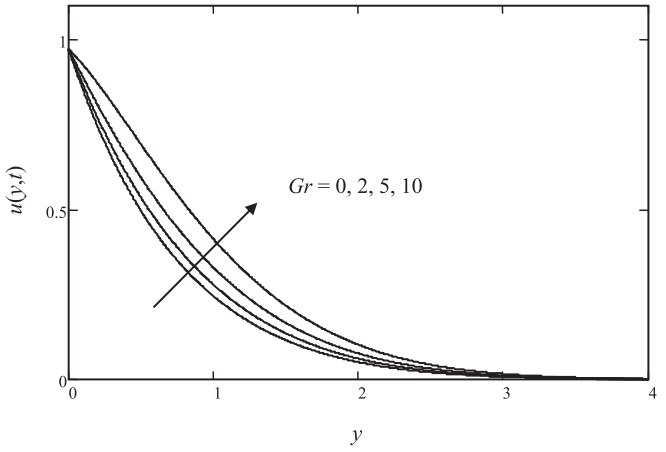

Fig. 3. Profiles of velocity for different values of *Gr*, when $\mathrm{Pr} = 0.3, \gamma = 0.6, M = 0.5, K = 0.2,\ t = 0.3$ and $\omega = \pi/4$.

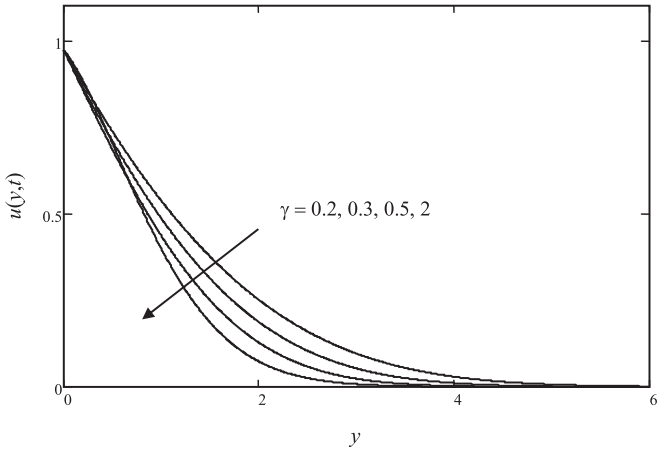

Fig. 4. Profiles of velocity for different values of γ, when $\mathrm{Pr} = 0.3, Gr = 0, M = 0.2, K = 2,\ t = 0.3$ and $\omega = \pi/4$.

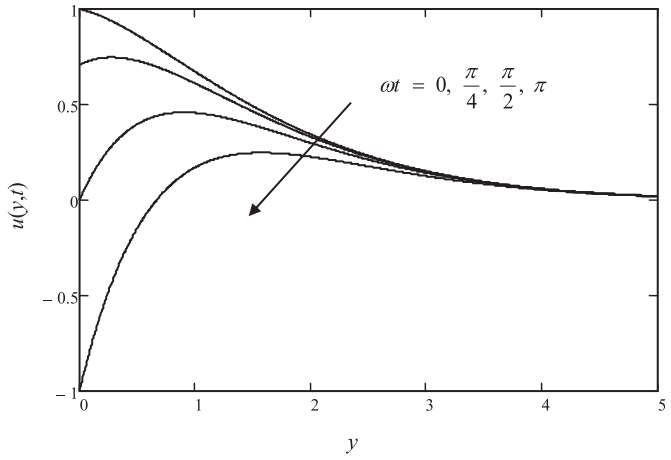

Fig. 5. Profiles of velocity for different values of ωt, when $Gr = 3$, $\Pr = 0.3, M = 0.5, K = 0.2, t = 1$ and $\gamma = 0.5$.

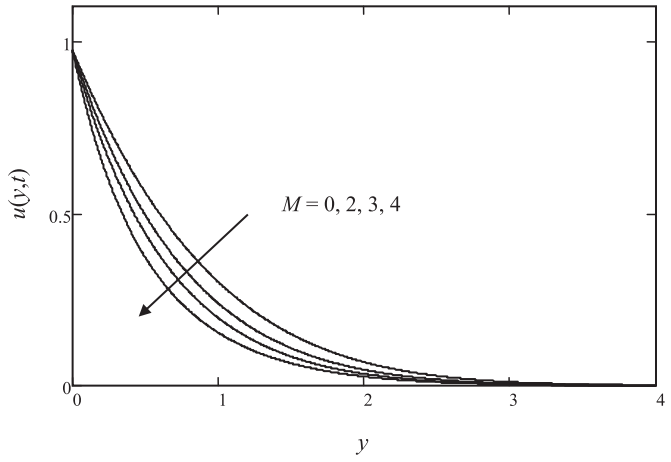

Fig. 6. Profiles of velocity for different values of M, when $\Pr = 0.3, Gr = 3$, $\gamma = 0.5, K = 0.2, t = 0.3$ and $\omega = \pi/4$.

increment in velocity boundary layer thickness. The graphical results for the phase angle ωt, are shown in Fig. 5. It is observed that the fluid is oscillating between -1 and 1. These fluctuations near the plate are maximum and decrease for further values of

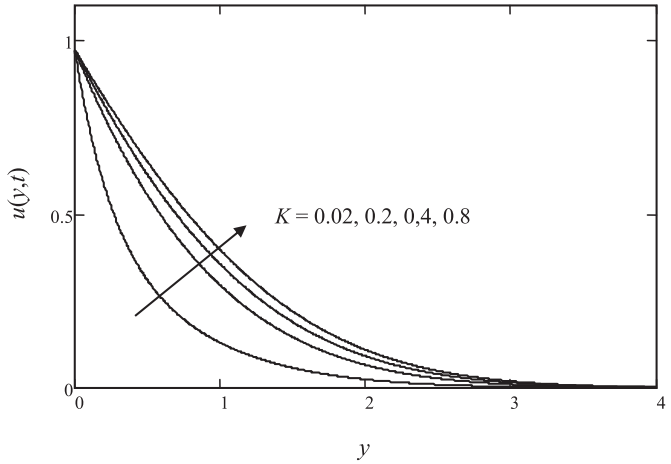

Fig. 7. Profiles of velocity for different values of K, when $\Pr = 0.3$, $Gr = 3$, $\gamma = 0.5, M = 0.5, t = 0.3$ and $\omega = \pi/4$.

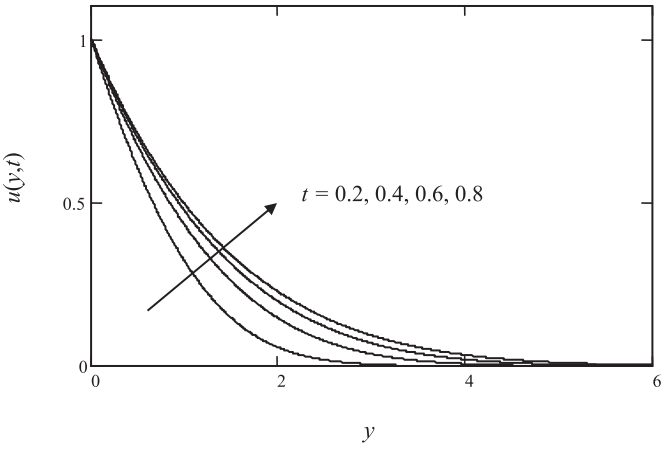

Fig. 8. Profiles of velocity for different values of t, when $\Pr = 0.3, Gr = 0$, $\gamma = 0.5, M = 0.5, K = 1$ and $\omega = 0$.

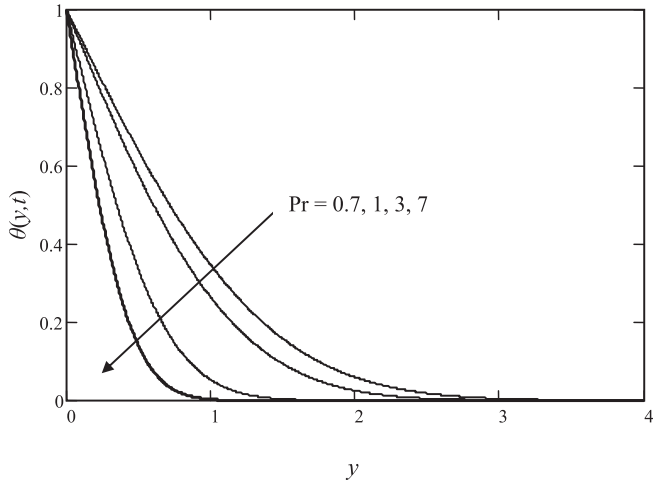

Fig. 9. Profiles of temperature for different values of Pr, when $t = 0.4$.

independent variable y. This figure can easily help us to check the accuracy of our results. For illustration of such results we have concentrated more on the values of $\omega t = 0$, $\pi/2$ and π. We can see that for these values of ωt, the velocity shows its value either 1,

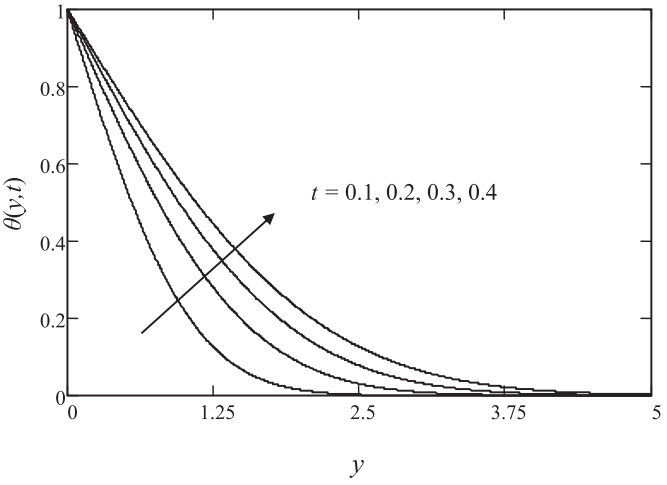

Fig. 10. Profiles of temperature for different values of t, when $\Pr = 0.71$.

Table 1
Skin-friction variations.

Pr	Gr	γ	ωt	M	K	t	τ
0.3	3	0.5	$\pi/4$	0.5	0.2	0.3	1.02992
0.71	3	0.5	$\pi/4$	0.5	0.2	0.3	1.29166
0.3	**5**	0.5	$\pi/4$	0.5	0.2	0.3	0.856995
0.3	3	**1.0**	$\pi/4$	0.5	0.2	0.3	0.93952
0.3	3	0.5	**$\pi/2$**	0.5	0.2	0.3	1.05009
0.3	3	0.5	$\pi/4$	**1.0**	0.2	0.3	1.08472
0.3	3	0.5	$\pi/4$	0.5	**1.0**	0.3	0.670207
0.3	3	0.5	$\pi/4$	0.5	0.2	**0.5**	0.692367

0 or −1 which are identical with the imposed boundary conditions of velocity in Equation (9). Hence, both the graphical and mathematical results are found in excellent agreement.

Fig. 6 displays the effect of magnetic parameter M on the velocity profiles. It is observed that the amplitude of the velocity as well as the boundary layer thickness decreases when M is increased. Physically, it may also be expected due to the fact that the application of a transverse magnetic field results in a resistive type force (called Lorentz force) similar to the drag force, and upon increasing the values of M, the drag force increases which leads to the deceleration of the flow. In Fig. 7, the profiles of velocity have been plotted for various values of permeability parameter K by keeping other parameters fixed. It is observed that for large values of K, velocity and boundary layer thickness increase which explains the physical situation that as K increases, the resistance of the porous medium is lowered which increases the momentum development of the flow regime, ultimately enhances the velocity field. In Fig. 8 the influence of dimensionless time t on the velocity profiles is shown. It is found that the velocity is an increasing function of time t.

It is depicted from Fig. 9 that, the temperature decreases as the Prandtl number Pr increases. It is justified due to the fact that thermal conductivity of the fluid decreases with increasing Prandtl number Pr and hence decreases the thermal boundary layer thickness. Fig. 10 is plotted to show the effects of the dimensionless time t on the temperature profiles. Four different values of time $t = 0.1$, $t = 0.2$, $t = 0.3$ and $t = 0.1$ are chosen. Obviously the temperature increases with increasing time t. This graphical behaviour of temperature is in good agreement with the corresponding boundary conditions of temperature profiles as shown in Equation (8). Results for skin-friction and Nusselt number are computed in Tables 1 and 2. The computations of skin-friction give complex results. Therefore, for the sake of convenience we have considered in Table 1 only its real part. The influence of Casson parameter on velocity and skin-friction is found identical with the published results of Mukhopadhyay [[23], see Figs. 3(a) and 7(a)]. Table 1 shows that skin-friction increases with increasing values of Pr and ωt whereas it decreases with increasing values of Gr, γ and t. On the other hand, it is found from Table 2 that Nusselt number increases with increasing Pr whereas decreases with increasing t. For the verification, we have compared our results with those of Fetecau et al. [31]. This comparison is shown in Fig. 11. It is found that our limiting solution (24) when $\gamma \to \infty$, (graph shown by solid line) are identical to Equation (8) (graph shown by filled squares) obtained by Fetecau et al. [31]. This confirms the accuracy of our obtained results. This figure further shows the comparison of velocity profiles in the absence as well as in the presence of MHD and porous medium. The graph for velocity when $M = 0.5$ and $K = 0.2$ are shown by filled circles whereas the graph for present velocity when $M = 1/K = 0$ are zero is given by solid line. It is clearly seen that the velocity decays early in the presence of MHD and porous medium.

Table 2
Nusstle number variations.

Pr	t	Nu
0.3	0.3	0.564
0.71	0.3	0.867
0.3	**0.6**	0.398

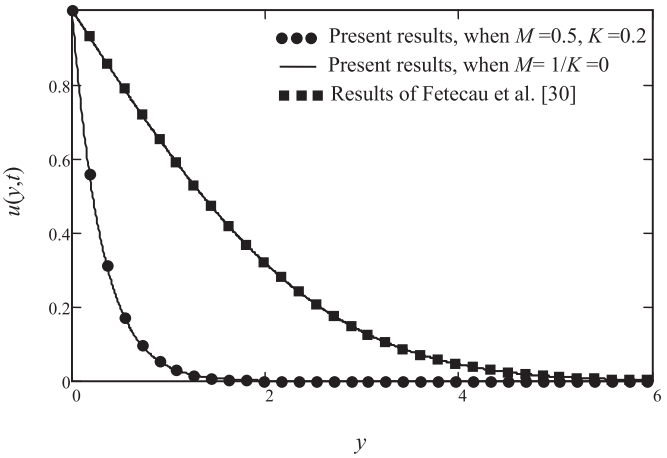

Fig. 11. Comparison of the present result [see Equation (24), when $\gamma \to \infty$] with that obtained by Fetecau et al. [31], [see Equation (8)], when $t = 0.2, \omega = 0, a = 1$, $U = 1$ and $\nu = 1$.

6. Conclusion

In this paper an exact analysis is performed to investigate the unsteady boundary layer flow of a Casson fluid past an oscillating vertical plate with constant wall temperature. The dimensionless governing equations are solved by using the Laplace transform technique. The results for velocity and temperature are obtained and plotted graphically. The numerical results for skin-friction and Nusselt number are computed in tables. The main conclusions of this study are as follows:

1. Velocity increases with increasing Gr, K and t whereas decreases with increasing values of Pr, M, γ and ωt.
2. Temperature increases with increasing t whereas decreases when Pr, is increased.
3. Skin-friction increases with increasing values of Pr,M and ωt whereas it decreases with increasing values of Gr, γ, K and t.
4. Nusselt number increases with increasing Pr whereas decreases with increasing t.
5. Solution (24) is found in excellent agreement with those obtained by Fetecau et al. [31].

Acknowledgments

The authors would like to acknowledge the SBKWU (HEC) Pakistan, Ministry of Education Malaysia (MOE) and Research Management Centre-UTM for the financial support through vote numbers 06H67 and 4F255 for this research.

References

[1] S. Nadeem, Rizwan Ul Haq, N.S. Akbar, Z.H. Khan, MHD three-dimensional Casson fluid flow past a porous linearly stretching sheet, Alexandria Eng. J. 52 (2013) 577–582.
[2] A. Mehmood, A. Ali, T. Mahmood, Unsteady magnetohydrodynamic oscillatory flow and heat transfer analysis of a viscous fluid in a porous channel filled with a saturated porous medium, J. Porous Media 13 (2010) 573–577.

[3] Nabil T.M. Eldabe, Galal M. Moatimid, Hoda S.M. Ali, Magnetohydrodynamic flow of non-Newtonian visco-elastic fluid through a porous medium near an accelerated plate, Can. J. Phys. 81 (2003) 1249–1269.
[4] Nabil T.M. Eldabe, S.N. Sallam, Non-Darcy couette flow through a porous medium of magnetohydrodynamic visco-elastic fluid with heat and mass transfer, Can. J. Phys. 83 (2005) 1241–1263.
[5] M. Hameed, S. Nadeem, Unstaedy MHD flow of a non-Newtonian fluid on a porous plate, J. Math. Anal. Appl. 325 (2007) 724–733.
[6] V. Rajesh, MHD effects on free convection and mass transform flow through a porous medium with variable temperature, Int. J. Appl. Math. Mech. 6 (2010) 1–16.
[7] M. Narahari, An exact solution of unsteady MHD free convection flow of a radiating gas past an infinite inclined isothermal plate, Appl. Mech. Mater. 110–116 (2012) 2228–2233.
[8] A.V. Kuznetsov, D.A. Nield, Natural convection boundary layer flow of a nanofluid past a vertical plate, Int. J. Therm. Sci. 40 (2001) 115–124.
[9] M. Turkyilmazoglu, I. Pop, Soret and heat source effects on the unsteady radiative MHD free convection flow from an impulsively started infinite vertical plate, Int. J. Heat Mass Transf. 55 (2012) 7635–7644.
[10] S. Sengupta, Thermal diffusion effect of free convection mass transfer flow past a uniformly accelerated porous plate with heat sink, Int. J. Math. Archive 2 (2011) 1266–1273.
[11] F. Ali, I. Khan and S. Shafie, Closed form solutions for unsteady free convection flow of a second grade fluid over an oscillating vertical plate, PLoS One 9(2): e85099. http://dx.doi.org/10.1371/journal.pone.0085099, PLoS ONE.
[12] I. Khan, F. Ali, S. Shafie, M. Qasim, Unsteady free convection flow in a Walters'-B fluid and heat transfer analysis, Bull. Malay. Math. Sci. Soc. (BMMS) 37 (2014) 437–448.
[13] Samiulhaq, A. Sohail, D. Vieru, I. Khan and S. Shafie, Unsteady magnetohydrodynamic free convection flow of a second grade fluid in a porous medium with ramped wall temperature, PLoS One 9(5): e88766. http://dx.doi.org/10.1371/journal.pone.0088766.
[14] N. Casson, A flow equation for the pigment oil suspensions of the printing ink type, in: Rheology of Disperse Systems, Pergamon, New York, 1959, pp. 84–102.
[15] K. Bhattacharyya, T. Hayat, A. Alsaedi, Exact solution for boundary layer flow of Casson fluid over a permeable stretching/shrinking sheet, Z. Angew. Math. Mech. 10 (2013) 1–7.
[16] R.K. Dash, K.N. Mehta, G. Jayaraman, Casson fluid flow in a pipe filled with a homogeneous porous medium, Int. J. Eng. Sci. 34 (1996) 1145–1156.
[17] Y.C. Fung, Biodynamics circulation, Springer-Verlag, New York, 1984.
[18] J. Boyd, J.M. Buick, S. Green, Analysis of the Casson and Carreau Yasuda non-Newtonian blood models in steady and oscillatory flow using the lattice Boltzmann method, Phys. Fluids 19 (2007). Article ID 093103.
[19] A.G. Fredrickson, Principles and applications of rheology, Prentice-Hall, Englewood Cliffs, N. J, 1964.
[20] A.V. Mernonr, J.N. Mazumdar, S.K. Lucas, A mathematical study of peristaltic transport of a Casson fluid, Math. Comput. Model. 35 (2002) 895–912.
[21] M. Mustafa, T. Hayat, I. Pop, A. Aziz, Unsteady boundary layer flow of a Casson fluid due to an impulsively started moving flat plate, Heat Transfer Asian Res. 40 (2011) 563–576.
[22] T. Hayat, S.A. Shehzad, A. Alsaedi, M.S. Alhothuali, Mixed convection stagnation point flow of Casson fluid with convective boundary conditions, Chin. Phys. Lett. 29 (2012). Article ID 114704.
[23] S. Shaw, P. Murthy, S.C. Pradhan, Effect of non-Newtonian characteristics of blood on magnetic targeting in the impermeable micro-vessel, J. Magn. Magn. Mater. 322 (2010) 1037–1043.
[24] S. Shaw, P. Murthy, Magnetic targeting in the impermeable microvessel with two-phase fluid model-Non-Newtonian characteristic of blood, Microvasc. Res. 80 (2010) 209–220.
[25] S. Shaw, R.S.R. Gorla, P. Murthy, C.O. Ng, Pulsatile Casson fluid flow through a stenosed bifurcated artery, Int. J. Fluid Mech. Res. 36 (2009).
[26] S. Mukhopadhyay, Effects of thermal radiation on Casson fluid flow and heat transfer over an unsteady stretching surface subjected to suction/blowing, Chin. Phys. B 22 (11) (2013). Article ID 114702.
[27] K. Bhattacharyya, Boundary layer stagnation-point flow of Casson fluid and heat transfer towards a shrinking/stretching sheet, Frontiers Heat Mass Transfer (FHMT) 4 (2013). Article ID 023003.
[28] S. Mukhopadhyay, P. De Rajan, K. Bhattacharyya, Casson fluid flow over an unsteady stretching surface, Ain Shams Eng. J. 4 (2013) 933–938.
[29] S. Pramanik, Casson fluid flow and heat transfer past an exponentially porous stretching surface in presence of thermal radiation, Ain Shams Eng. J. 5 (2014) 205–212.
[30] S. Kim, Study of non-Newtonian viscosity and yield stress of blood in a scanning capillary-tube rheometer. (A), Ph.D. dissertation, Mech. Eng. Mech. (2002).
[31] M. Nakamura, T. Sawada, Numerical study on the flow of a non-Newtonian fluid through an axisymmetric stenosis, ASME J. Biomech. Eng. 110 (1988) 137–143.
[32] K. Bhattacharyya, T. Hayat, A. Alsaedi, Analytic solution for magnetohydrodynamic boundary layer flow of Casson fluid over a stretching/shrinking sheet with wall mass transfer, Chin. Phys. B 22 (2013). Article ID 024702.
[33] Corina Fetecau, D. Vieru, C. Fetecau, A note on the second problem of stokes for Newtonian fluids, Int. J. Nonlinear Mech. 43 (2008) 451–457.
[34] A. Hussanan, Z. Ismail, I. Khan, A.G. Hussein, S. Shafie, Unsteady boundary layer MHD free convection flow in a porous medium with constant mass diffusion and Newtonian heating, Eur. Phys. J. Plus 129 (2014) 46.
[35] F. Ali, I. Khan, Samiulhaq, S. Shafie, A note on new exact solutions for some unsteady flows of Brinkman-type fluids over a plane wall, Verlag der Zeitschrift für Naturforschung 67 (2012) 377–380.
[36] A. Hussanan, I. Khan, and S. Shafie, An exact analysis of heat and mass transfer past a vertical plate with Newtonian heating. Journal of Applied Mathematics, volume 2013, Article ID 434571, 9 pages.